EUROPEAN ORGANISATION FOR PARTICLE PHYSICS

CERN-PPE/93-67
30th April 1993

Search for Anomalous Production of High Mass Photon Pairs in e^+e^- Collisions at LEP

The OPAL Collaboration

Abstract

A search for events with photon pairs of large invariant mass is described based on a data sample of 43 pb^{-1} collected with the OPAL detector. This search is motivated by the L3 observation of four events of the type $e^+e^- \to \ell^+\ell^-\gamma\gamma$ with an invariant mass of the two photons, $m_{\gamma\gamma}$, clustering around 60 GeV. In the OPAL data, four $\ell^+\ell^-\gamma\gamma$ events are found with $m_{\gamma\gamma}$ above 40 GeV. The number of observed events is consistent with the QED expectation and no obvious resonance structure is seen. Three candidate $q\bar{q}\gamma\gamma$ events with $m_{\gamma\gamma}$ above 40 GeV are found and no $\nu\bar{\nu}\gamma\gamma$ candidate with $m_{\gamma\gamma} > 5$ GeV is found. From these searches an upper limit is set on any anomalous production of $\ell^+\ell^-\gamma\gamma(\ell = e, \mu, \tau)$ events, where the $\ell^+\ell^-$ pair comes from a virtual Z^0 and $m_{\gamma\gamma}$ is near 60 GeV, of $B(Z^0 \to Z^{*0}\gamma\gamma \to \ell^+\ell^-\gamma\gamma) < 6.0 \times 10^{-7}$ at the 95% C.L. In a similar search in the reaction $e^+e^- \to \gamma\gamma\gamma$, seven events are observed with a photon pairing of mass near 60 GeV compared to an expected background of 2.7 ± 0.4 from QED. In a search for the production of a 60 GeV resonance X in two-photon collisions, an upper limit is set on $\Gamma_X B^2(X \to \gamma\gamma)$ of 2.6 MeV at the 95% C.L. A search is also performed for $\ell^+\ell^- X(\ell = e, \mu)$ events in non-$\gamma\gamma$ decay modes of X. No indication of a 60 GeV resonance is seen. Combining these two searches, Γ_X values greater than 110 MeV are excluded at the 95% C.L. for $\ell^+\ell^-\gamma\gamma(\ell = e, \mu)$ cross-sections greater than 0.05 pb.

(Submitted to Physics Letters B)

The OPAL Collaboration

P.D. Acton[25], R. Akers[16], G. Alexander[23], J. Allison[16], K.J. Anderson[9], S. Arcelli[2], A. Astbury[28], D. Axen[29], G. Azuelos[18,a], J.T.M. Baines[16], A.H. Ball[17], J. Banks[16], R.J. Barlow[16], S. Barnett[16], R. Bartoldus[3], J.R. Batley[5], G. Beaudoin[18], A. Beck[23], G.A. Beck[13], J. Becker[10], C. Beeston[16], T. Behnke[27], K.W. Bell[20], G. Bella[23], P. Bentkowski[18], P. Berlich[10], S. Bethke[11], O. Biebel[3], I.J. Bloodworth[1], P. Bock[11], B. Boden[3], H.M. Bosch[11], M. Boutemeur[18], H. Breuker[8], P. Bright-Thomas[25], R.M. Brown[20], A. Buijs[8], H.J. Burckhart[8], C. Burgard[27], P. Capiluppi[2], R.K. Carnegie[6], A.A. Carter[13], J.R. Carter[5], C.Y. Chang[17], D.G. Charlton[8], S.L. Chu[4], P.E.L. Clarke[25], J.C. Clayton[1], I. Cohen[23], J.E. Conboy[15], M. Cooper[22], M. Coupland[14], M. Cuffiani[2], S. Dado[22], G.M. Dallavalle[2], S. De Jong[13], L.A. del Pozo[5], H. Deng[17], A. Dieckmann[11], M. Dittmar[4], M.S. Dixit[7], E. do Couto e Silva[12], J.E. Duboscq[8], E. Duchovni[26], G. Duckeck[11], I.P. Duerdoth[16], D.J.P. Dumas[6], P.A. Elcombe[5], P.G. Estabrooks[6], E. Etzion[23], H.G. Evans[9], F. Fabbri[2], B. Fabbro[21], M. Fierro[2], M. Fincke-Keeler[28], H.M. Fischer[3], D.G. Fong[17], M. Foucher[17], A. Gaidot[21], J.W. Gary[4], J. Gascon[18], N.I. Geddes[20], C. Geich-Gimbel[3], S.W. Gensler[9], F.X. Gentit[21], G. Giacomelli[2], R. Giacomelli[2], V. Gibson[5], W.R. Gibson[13], J.D. Gillies[20], J. Goldberg[22], D.M. Gingrich[30,a], M.J. Goodrick[5], W. Gorn[4], C. Grandi[2], F.C. Grant[5], J. Hagemann[27], G.G. Hanson[12], M. Hansroul[8], C.K. Hargrove[7], P.F. Harrison[13], J. Hart[8], P.M. Hattersley[1], M. Hauschild[8], C.M. Hawkes[8], E. Heflin[4], R.J. Hemingway[6], G. Herten[10], R.D. Heuer[8], J.C. Hill[5], S.J. Hillier[8], T. Hilse[10], D.A. Hinshaw[18], J.D. Hobbs[8], P.R. Hobson[25], D. Hochman[26], R.J. Homer[1], A.K. Honma[28,a], R.E. Hughes-Jones[8], R. Humbert[10], P. Igo-Kemenes[11], H. Ihssen[11], D.C. Imrie[25], A.C. Janissen[6], A. Jawahery[17], P.W. Jeffreys[20], H. Jeremie[18], M. Jimack[1], M. Jones[29], R.W.L. Jones[8], P. Jovanovic[1], C. Jui[4], D. Karlen[6], K. Kawagoe[24], T. Kawamoto[24], R.K. Keeler[28], R.G. Kellogg[17], B.W. Kennedy[15], S. Kluth[5], T. Kobayashi[24], D.S. Koetke[8], T.P. Kokott[3], S. Komamiya[24], L. Köpke[8], J.F. Kral[8], R. Kowalewski[6], J. von Krogh[11], J. Kroll[9], M. Kuwano[24], P. Kyberd[13], G.D. Lafferty[16], H. Lafoux[21], R. Lahmann[17], F. Lamarche[18], J.G. Layter[4], P. Leblanc[18], A.M. Lee[31], M.H. Lehto[15], D. Lellouch[26], C. Leroy[18], J. Letts[4], S. Levegrün[3], L. Levinson[26], S.L. Lloyd[13], F.K. Loebinger[16], J.M. Lorah[17], B. Lorazo[18], M.J. Losty[7], X.C. Lou[12], J. Ludwig[10], A. Luig[10], M. Mannelli[8], S. Marcellini[2], C. Markus[3], A.J. Martin[13], J.P. Martin[18], T. Mashimo[24], P. Mättig[3], U. Maur[3], J. McKenna[28], T.J. McMahon[1], J.R. McNutt[25], F. Meijers[8], D. Menszner[11], F.S. Merritt[9], H. Mes[7], A. Michelini[8], R.P. Middleton[20], G. Mikenberg[26], J. Mildenberger[6], D.J. Miller[15], R. Mir[12], W. Mohr[10], C. Moisan[18], A. Montanari[2], T. Mori[24], M. Morii[24], U. Müller[3], B. Nellen[3], H.H. Nguyen[9], S.W. O'Neale[1], F.G. Oakham[7], F. Odorici[2], H.O. Ogren[12], C.J. Oram[28,a], M.J. Oreglia[9], S. Orito[24], J.P. Pansart[21], B. Panzer-Steindel[8], P. Paschievici[26], G.N. Patrick[20], N. Paz-Jaoshvili[23], M.J. Pearce[1], P. Pfister[10], J.E. Pilcher[9], J. Pinfold[30], D. Pitman[28], D.E. Plane[8], P. Poffenberger[28], B. Poli[2], A. Pouladdej[6], T.W. Pritchard[13], H. Przysiezniak[18], G. Quast[27], M.W. Redmond[8], D.L. Rees[8], G.E. Richards[16], S.A. Robins[13], D. Robinson[8], A. Rollnik[3], J.M. Roney[28,b], E. Ros[8], S. Rossberg[10], A.M. Rossi[2], M. Rosvick[28], P. Routenburg[6], K. Runge[10], O. Runolfsson[8], D.R. Rust[12], M. Sasaki[24], C. Sbarra[2], A.D. Schaile[10], O. Schaile[10], W. Schappert[6], P. Scharff-Hansen[8], P. Schenk[4], B. Schmitt[3], H. von der Schmitt[11], M. Schröder[12], C. Schwick[27], J. Schwiening[3], W.G. Scott[20], M. Settles[12], T.G. Shears[5], B.C. Shen[4], C.H. Shepherd-Themistocleous[7], P. Sherwood[15], G.P. Siroli[2], A. Skillman[16], A. Skuja[17], A.M. Smith[8], T.J. Smith[28], G.A. Snow[17], R. Sobie[28,b], R.W. Springer[17], M. Sproston[20], A. Stahl[3], C. Stegmann[10], K. Stephens[16], J. Steuerer[28], R. Ströhmer[11], D. Strom[19], H. Takeda[24], T. Takeshita[24,c], S. Tarem[26], M. Tecchio[9], P. Teixeira-Dias[11], N. Tesch[3], M.A. Thomson[15], E. Torrente-Lujan[22], S. Towers[28], G. Transtromer[25], N.J. Tresilian[16], T. Tsukamoto[24], M.F. Turner[8], D. Van den plas[18], R. Van Kooten[27], G.J. VanDalen[4], G. Vasseur[21], C.J. Virtue[7], A. Wagner[27], D.L. Wagner[9], C. Wahl[10], C.P. Ward[5], D.R. Ward[5], P.M. Watkins[1], A.T. Watson[1], N.K. Watson[8], M. Weber[11], P. Weber[6], P.S. Wells[8], N. Wermes[3], M.A. Whalley[1], B. Wilkens[10], G.W. Wilson[4], J.A. Wilson[1], V-H. Winterer[10], T. Wlodek[26], G. Wolf[26], S. Wotton[11], T.R. Wyatt[16], R. Yaari[26], A. Yeaman[13], G. Yekutieli[26], M. Yurko[18], W. Zeuner[8], G.T. Zorn[17].

[1]School of Physics and Space Research, University of Birmingham, Birmingham, B15 2TT, UK
[2]Dipartimento di Fisica dell' Università di Bologna and INFN, Bologna, 40126, Italy
[3]Physikalisches Institut, Universität Bonn, D-5300 Bonn 1, Germany
[4]Department of Physics, University of California, Riverside, CA 92521 USA
[5]Cavendish Laboratory, Cambridge, CB3 0HE, UK
[6]Carleton University, Dept of Physics, Colonel By Drive, Ottawa, Ontario K1S 5B6, Canada
[7]Centre for Research in Particle Physics, Carleton University, Ottawa, Ontario K1S 5B6, Canada
[8]CERN, European Organisation for Particle Physics, 1211 Geneva 23, Switzerland
[9]Enrico Fermi Institute and Dept of Physics, University of Chicago, Chicago Illinois 60637, USA
[10]Fakultät für Physik, Albert Ludwigs Universität, D-7800 Freiburg, Germany
[11]Physikalisches Institut, Universität Heidelberg, Heidelberg, Germany
[12]Indiana University, Dept of Physics, Swain Hall West 117, Bloomington, Indiana 47405, USA
[13]Queen Mary and Westfield College, University of London, London, E1 4NS, UK
[14]Birkbeck College, London, WC1E 7HV, UK
[15]University College London, London, WC1E 6BT, UK
[16]Department of Physics, Schuster Laboratory, The University, Manchester, M13 9PL, UK
[17]Department of Physics, University of Maryland, College Park, Maryland 20742, USA
[18]Laboratoire de Physique Nucléaire, Université de Montréal, Montréal, Quebec, H3C 3J7, Canada
[19]University of Oregon, Dept of Physics, Eugene, Oregon 97403, USA
[20]Rutherford Appleton Laboratory, Chilton, Didcot, Oxfordshire, OX11 0QX, UK
[21]DAPNIA/SPP, Saclay, F-91191 Gif-sur-Yvette, France
[22]Department of Physics, Technion-Israel Institute of Technology, Haifa 32000, Israel
[23]Department of Physics and Astronomy, Tel Aviv University, Tel Aviv 69978, Israel
[24]International Centre for Elementary Particle Physics and Dept of Physics, University of Tokyo, Tokyo 113, and Kobe University, Kobe 657, Japan
[25]Brunel University, Uxbridge, Middlesex, UB8 3PH UK
[26]Nuclear Physics Department, Weizmann Institute of Science, Rehovot, 76100, Israel
[27]Universität Hamburg/DESY, II Inst für Experimental Physik, 2000 Hamburg 52, Germany
[28]University of Victoria, Dept of Physics, P O Box 3055, Victoria BC V8W 3P6, Canada
[29]University of British Columbia, Dept of Physics, Vancouver BC V6T 1Z1, Canada
[30]University of Alberta, Dept of Physics, Edmonton AB T6G 2N5, Canada
[31]Duke University, Dept of Physics, Durham, North Carolina 27708-0305, USA

[a]Also at TRIUMF, Vancouver, Canada V6T 2A3
[b]And IPP, University of Victoria, Dept of Physics, P O Box 3055, Victoria BC V8W 3P6, Canada
[c]Also at Shinshu University, Matsumoto 390, Japan

1 Introduction

The L3 collaboration has observed [1] four $\ell^+\ell^-\gamma\gamma$ events (three $\mu^+\mu^-\gamma\gamma$ and one $e^+e^-\gamma\gamma$) where the two energetic photons have a mass $m_{\gamma\gamma}$ near 60 GeV, within a data sample of about 0.95 million produced Z^0's. The invariant masses of the two photon system for the four events are 58.8, 59.0, 62.0 and 60.0 GeV with a mass resolution of 0.6 GeV. The QED background was estimated using the YFS3 Monte Carlo [2] and a probability of order 10^{-3} was calculated for the observation of four or more events in any 5 GeV mass interval above 50 GeV. L3 has also searched for events of the type $q\bar{q}\gamma\gamma$ and $\nu\bar{\nu}\gamma\gamma$, but no event with a high mass photon pair was found. Recently, L3 has updated the result with a larger data sample of 1.6 million produced Z^0's [3]: no additional $\ell^+\ell^-\gamma\gamma$ event near 60 GeV was found and the probability of a QED fluctuation as calculated above is of order 10^{-2}. Several authors have recently repeated or calculated independently the QED expectation [4]. The L3 publication has motivated the other LEP experiments to look for such events [5], and experiments at TRISTAN to scan in the 60 GeV energy region. The results from TRISTAN [6] exclude a large coupling to electrons of a possible new particle.

The L3 publication has led to various phenomenological models being considered or advocated as potential sources of anomalous $\ell^+\ell^-\gamma\gamma$ events. Besides a more general consideration of various possibilities [7], these models include multi-Higgs doublet models [8, 9], Z′ with coupling only to right-handed fermions [10], heavy axions [11] and pseudo-goldstone bosons in a technicolour model [12]. The phenomenology at lower energies assuming a leptonic coupling is discussed in [13].

OPAL has published the first detailed measurements at LEP of photon bremsstrahlung from quarks [14] and from charged leptons [15] and also of single photon counting [16]. In this paper we describe the results of the OPAL search for events with two energetic photons of high invariant mass using the entire data sample collected between 1990 and 1992. The data sample of about 43 pb^{-1} corresponds to a total of 1.8 million produced Z^0 events.

The search for high mass photon pairs in charged leptonic events is described in section 3. If the photon pairs are produced in association with a virtual Z^0 decaying to a lepton pair, they should also be observable in events where the virtual Z^0 decays to $q\bar{q}$ or $\nu\bar{\nu}$. Events of the type $q\bar{q}\gamma\gamma$ could also be produced with a comparable production rate if the lepton pair comes from a virtual photon. In section 4 we describe the search for high mass photon pairs in hadronic events and in events without charged particles. Motivated by the possible production in association with a real photon, we search for high mass photon pairs in $e^+e^- \to \gamma\gamma\gamma$ events (section 5). In section 6 we also look for the production via two-photon collisions of a resonant state decaying to two photons in the no charged particle topology. Finally, in section 7, we search for events with an isolated high momentum charged lepton pair in the $\ell^+\ell^-q\bar{q}$, $\ell^+\ell^-\ell^+\ell^-$ or $\ell^+\ell^-\nu\bar{\nu}$ topologies. The motivation for this study is to search for a resonance state X with a mass of about 60 GeV that can be produced together with a lepton pair in e^+e^- annihilation and has decay modes other than $X \to \gamma\gamma$.

2 OPAL detector

The OPAL detector which is described in detail in [17] is a solenoidal detector with a pressurised central tracking system operating in a 0.435 T magnetic field. The lead-glass electromagnetic calorimeter together with presamplers and time-of-flight (TOF) scintillators is located outside the magnet coil and pressure vessel. The magnet return yoke is instrumented for hadron calorimetry and is surrounded by

external muon chambers. Calorimeters close to the beam axis[1] measure luminosity and complete the acceptance. The detector features of relevance to this analysis are described briefly below.

The central tracking system consists of a vertex drift chamber, a jet chamber, z-chambers and a silicon micro-vertex detector. In the range $|\cos\theta| < 0.73$, 159 points are measured in the jet chamber along each track and at least 20 points on a track are obtained over 96% of the full solid angle. The momentum in the r-ϕ plane, p_t, is measured with a resolution of $(\sigma(p_t)/p_t)^2 = 0.02^2 + (0.0015 \cdot p_t)^2$, ($p_t$ in GeV) for $|\cos\theta| < 0.7$. The photon conversion probability arising from the material of the beampipe and the central tracking detector is about 8% in the barrel region.

The TOF scintillation counters are located immediately after the coil in the barrel region. Most photons (80%) convert in the coil and are measured with a time resolution of better than 300 ps. The barrel presampler detector consists of a cylinder of limited streamer tubes located between the TOF and the barrel lead-glass calorimeter and is used to obtain a precise angular measurement of the photon. The angular resolution in each spherical co-ordinate for high energy photons is about 2 mrad.

Photon energies are measured by the barrel and endcap lead-glass electromagnetic calorimeters. These detectors cover the full azimuthal angular range in the polar angle range of $|\cos\theta| < 0.82$ for the barrel and $0.81 < |\cos\theta| < 0.984$ for the endcaps. The forward detectors on both sides of the interaction point cover the polar angle region between 34 and 120 mrad. When high energy electrons or photons are incident on the gap of 0.8% in solid angle between the endcap lead-glass and the forward detector, some fraction of the shower is usually detected at the edge of one of these calorimeters. Thus, photons and electrons are detected with an acceptance of almost 4π. The barrel lead-glass blocks have a pointing geometry. To achieve good hermeticity, the small 1 mm gaps between the lead-glass blocks do not point exactly to the interaction point. The intrinsic energy resolution of the calorimeter is $5\text{–}6\%/\sqrt{E}$ which is degraded by about a factor of two by the material of the magnet coil and the pressure vessel in front of the calorimeter. The effect of material is more significant in the region near the overlap of the barrel and the endcap calorimeters ($0.72 < |\cos\theta| < 0.82$), hereafter referred to as the "overlap region". The angular resolution of electromagnetic clusters is approximately 4 mrad both in θ and ϕ for energies above 10 GeV. From studies using planar $e^+e^- \to \ell^+\ell^-\gamma$ (ℓ = e or μ) events and collinear $e^+e^- \to \gamma\gamma$ events, one concludes that the mass resolution, for $m_{\gamma\gamma}$ between 50-70 GeV, is typically 2 GeV. Full efficiency at the trigger level [18] is achieved for all channels studied (including the topology of no charged tracks).

3 Search for charged lepton pair events with isolated energetic photons

In the following we search for events with at least two isolated photons and a charged lepton pair.

3.1 $\ell^+\ell^-\gamma\gamma(\ell = e, \mu, \tau)$ events

Two independent but similar searches for $\ell^+\ell^-\gamma\gamma$ events have been performed. The lepton selection is based on low charged multiplicity jets [19]. Starting from energetic tracks, geometric cones, with opening angles between 10–35° depending on the specific analysis goals, are used to combine close by tracks and clusters into jets. The events of interest are identified as having exactly two such charged

[1] A spherical polar co-ordinate system is used with the polar angle θ defined relative to the electron beam direction (z).

jets and at least two isolated energetic electromagnetic clusters without associated charged particles. These clusters are considered to be photons. In order to have good electromagnetic energy resolution, photons in the overlap region are not considered.

The criteria for the first analysis require that one charged jet is found within $|\cos\theta| < 0.7$ and the second one within $|\cos\theta| < 0.94$. At least two photons are required to be within $|\cos\theta| < 0.94$. The criteria are described in detail in our previous publication [15].

The second analysis has a somewhat larger acceptance for charged leptons and a slightly reduced acceptance for photons. The analysis starts from a sample with a charged multiplicity between 2 and 6, and a minimum visible energy (scalar sum of the charged particle momenta and electromagnetic cluster energies) of 10% of the centre-of-mass energy. Low multiplicity charged jets are defined by a cone of 10° half-angle. The jets and photons are each required to have an energy of more than 2 GeV and be detected within $|\cos\theta| < 0.9$. Photon pairings are considered if the photons are separated by more than 10° from each other and each jet.

The same four events with a two-photon invariant mass above 40 GeV are found by both selections: two $\mu^+\mu^-\gamma\gamma$ and two $e^+e^-\gamma\gamma$ events. The lepton flavour of each charged jet is assigned as an electron using track-cluster energy matching, or as a muon using identification criteria based on the OPAL Z^0 lineshape analysis [20]. Events with charged jets of unassigned or mixed flavour and events with large missing energy are called $\tau^+\tau^-$. The measured 4-vectors of the events are given in Table 1. These events are discussed in more detail in section 3.2. The mass spectrum $m_{\gamma\gamma}$ of the highest mass photon pair for all the events selected in the latter analysis is shown in Figure 1(a). The mass is calculated from the calorimeter energy and only a few events at low mass have more than two accepted photons.

In order to compare with the YFS3 Monte Carlo (MC) [2], which is currently only available for muon pair production with multiple hard photons, we selected events with $\mu^+\mu^-$ from the above sample. The $m_{\gamma\gamma}$ distribution for events with $\mu^+\mu^-$ is shown in Figure 1(b), together with the YFS3 MC expectation with full detector simulation [21]. We observe 29 events with $m_{\gamma\gamma}$ above 10 GeV which is consistent with the YFS3 MC prediction of 22.6 ± 1.2. Two events are seen with $m_{\gamma\gamma}$ above 40 GeV compared with the Monte Carlo prediction of 1.2 ± 0.3.

The overall detection efficiencies for $e^+e^- \to e^+e^-X$, $\mu^+\mu^-X$ and $\tau^+\tau^-X$ events with X decaying to $\gamma\gamma$ and $m_X = 60$ GeV are $46 \pm 3\%$, $54 \pm 3\%$ and $22 \pm 2\%$, respectively, where the error is mainly due to Monte Carlo statistics and uncertainties on the photon conversion rate. These efficiencies are calculated by using a Monte Carlo with full detector simulation assuming the same production angular distribution as for a standard model Higgs boson ($e^+e^- \to Z^{*0}H^0$) for X and subsequent isotropic decay into $\gamma\gamma$ [22]. Efficiencies for X production accompanied by other fermion pairs (section 4) and those for X decaying into fermion pairs (section 7) are also calculated using this model. We have investigated possible model dependence. The case of a particle of 60 GeV mass emitted in a bremsstrahlung-like manner from a lepton has been shown to be essentially the same as for $Z^{*0}H^0$. The efficiency drops by only a factor of 0.87 for an extreme case in which the production angle of X peaks at large $|\cos\theta|$, arbitrarily chosen as $|Y_2{}^0|^2$ $((3\cos^2\theta - 1)^2)$, and at the same time the $\gamma\gamma$ decay angle distribution with respect to the X flight direction peaks forward and backward as $|Y_2{}^0|^2$.

3.2 Detailed studies of the four $\ell^+\ell^-\gamma\gamma$ events with high two photon invariant mass

In this section we discuss some checks of the two photon mass measurement in these four events and consider possible improvements to the mass resolution. These checks involve all four measured particles and we clarify how the four-vectors of Table 1 have been measured. The tracking chambers

Table 1: List of four-vectors for the events with $m_{\gamma\gamma} > 40$ GeV. The photon energies given are the direct measurements.

Event	A	B	C	D
Event type	$\mu^+\mu^-\gamma\gamma$	$e^+e^-\gamma\gamma$	$e^+e^-\gamma\gamma$	$\mu^+\mu^-\gamma\gamma$
$\sqrt{s}$ (GeV)	91.244	89.250	91.237	92.966
$E_{\gamma 1}$ (GeV)	30.9	36.8	43.2	41.7
$\cos\theta_{\gamma 1}$	0.578	0.249	−0.498	−0.625
$\phi_{\gamma 1}$ (°)	52.8	93.5	85.7	255.1
$E_{\gamma 2}$ (GeV)	24.6	20.7	15.8	10.6
$\cos\theta_{\gamma 2}$	−0.469	−0.630	0.154	0.560
$\phi_{\gamma 2}$ (°)	214.5	281.1	239.0	66.9
$p_{\ell 1}$ (GeV)	20.8	13.1	21.7	29.1
$\cos\theta_{\ell 1}$	−0.627	−0.198	0.773	0.715
$\phi_{\ell 1}$ (°)	227.4	262.0	284.1	98.8
$p_{\ell 2}$ (GeV)	15.9	8.2	7.3	9.0
$\cos\theta_{\ell 2}$	0.444	0.343	−0.092	−0.027
$\phi_{\ell 2}$ (°)	16.5	276.8	280.2	20.2

are used for the measurement of the lepton angles and the muon momenta. The leptons are fitted to a common vertex consistent with the beam spot. The energies of the photons and electrons are measured by the electromagnetic calorimeter. If the electron extrapolates into the overlap region then the track momentum is used (lepton 1 in event C). The photon angles relative to the vertex are measured using the presampler in preference to the calorimeter if one presampler cluster can be unambiguously associated with the calorimeter cluster.

As discussed above, the lead glass calorimeter is estimated to give accuracies for the $m_{\gamma\gamma}$ system of about 2 GeV for masses of 60 GeV. The invariant mass of the two photon system can also be estimated independently from the recoil mass of the two leptons assuming a four-body final state. The different mass estimates are summarised in Table 2.

When all particles in an event are completely reconstructed, kinematic fitting with the four constraints of energy and momentum conservation is a powerful technique that can greatly improve the mass resolution. This technique is inappropriate for events with tau leptons because of the unreconstructed neutrinos. In e^+ e^- collisions, these fits must consider the possibility of single and multiple initial state radiation (ISR) which lead to unobserved photons close to the beam axis. Even if all the particles are within the detector acceptance, full reconstruction is not guaranteed because collinear photons may not be identified experimentally and soft photons ($E < O(300$ MeV)) are not detected with full efficiency. We carry out three kinematic fits. Firstly we fit the event to the four-body hypothesis and secondly to a hypothesis allowing ISR photons emitted along the beam axis in one hemisphere with an arbitrary energy. The first fit has the four constraints of four-momentum conservation while the second one has three constraints because of the ISR ambiguity. In the third fit, which has two constraints, we allow any number of ISR photons of arbitrary energy produced parallel to the beam direction in both hemispheres.

We have checked our method by kinematic fitting of a sample of electron and muon pair events with at least one isolated photon. We find that 56% of these events can be satisfactorily described using the 4C fit while 22% require ISR photons in one hemisphere (3C fit) to give an acceptable fit. Only 1% of the events require the 2C fit. The remaining 21% do not fit at all: there are indications from the unassociated energy in the calorimeter and the planarity that these events have additional

Table 2: List of $\gamma\gamma$ invariant masses for $\ell^+\ell^-\gamma\gamma$ events with $m_{\gamma\gamma} > 40$ GeV. $m_{\gamma\gamma}$(recoil) is the recoil mass of the two leptons. $m_{\gamma\gamma}$(4C fit, no ISR) is obtained with the four body kinematic fit, and $m_{\gamma\gamma}$(3C fit, with 1 ISR) is the fit allowing ISR photons in one hemisphere. $m_{\gamma\gamma}$(2C fit, multiple ISR) is the fit allowing ISR photons in both hemispheres. The measured visible energy, $E_{\rm vis}$ (sum of charged particle energies and photon energies), is also listed in the table. Negative values of E_{ISR} indicate that the ISR photon is emitted along the $-z$ direction.

Event	A	B	C	D
Event type	$\mu^+\mu^-\gamma\gamma$	$e^+e^-\gamma\gamma$	$e^+e^-\gamma\gamma$	$\mu^+\mu^-\gamma\gamma$
$\sqrt{s}$ (GeV)	91.244	89.250	91.237	92.966
$E_{\rm vis}$ (GeV)	92.3 ± 2.3	78.7 ± 2.5	88.0 ± 2.6	90.4 ± 2.5
$m_{\gamma\gamma}$ (GeV)	54.6 ± 2.1	53.8 ± 2.1	50.1 ± 2.0	41.9 ± 1.9
$m_{\gamma\gamma}$(recoil) (GeV)	53.5 ± 0.8	64.9 ± 1.5	56.3 ± 1.6	45.0 ± 2.0
$m_{\gamma\gamma}$(4C fit, no ISR) (GeV)	53.3 ± 0.4	56.0 ± 0.3	49.9 ± 0.4	43.6 ± 0.9
χ^2/d.o.f.	5.7/4	37/4	12.9/4	11.6/4
$m_{\gamma\gamma}$(3C fit, with 1 ISR) (GeV)	53.8 ± 0.4	58.3 ± 0.4	49.6 ± 0.5	42.3 ± 1.0
E_{ISR} (GeV)	-0.4 ± 0.2	3.7 ± 0.6	0.9 ± 0.6	-0.8 ± 0.3
χ^2/d.o.f.	1.0/3	7.6/3	9.0/3	1.6/3
$m_{\gamma\gamma}$(2C fit, multiple ISR) (GeV)	53.7 ± 0.4	53.7 ± 1.9	46.8 ± 1.4	41.5 ± 1.8
χ^2/d.o.f.	1.0/2	0.1/2	5.8/2	1.4/2

photons and are not three-body events. Correspondingly, one expects that a similar significant fraction of the $\ell^+\ell^-\gamma\gamma$ events will not give a reasonable fit. For the events which have a reasonable 4C fit, the fit probability distribution and the pull distributions for each measured quantity are as expected, confirming the reliability of the error estimates. The fit results for the $\ell^+\ell^-\gamma\gamma$ events are also shown in Table 2. For three of the events the fitted mass in the 3C fit is in good agreement with the direct measurement.

In event B, which is measured at $\sqrt{s} = m_{Z^0} - 2$ GeV, the 4C fit gives an unacceptable description as also indicated by the recoil mass calculation. Inspection of this event reveals that there is a significant deposit of energy (400 MeV) at the inner edge of the endcap electromagnetic calorimeter in the same hemisphere as the missing momentum. The 3C fit with ISR in one hemisphere has an adequate χ^2 (5% probability) while the hypothesis of double initial state radiation (2C fit) gives a much better agreement between measured and fitted quantities. This is a consequence of the measured transverse momentum being well balanced, which also disfavours an interpretation as $\tau^+\tau^-\gamma\gamma$. We note that for $\sqrt{s} = m_{Z^0} - 2$ GeV, the emission of hard ISR photons in both hemispheres occurs with a probability of a few percent relative to the rate for emission of hard ISR photons in a single hemisphere. The interpretation of this event is ambiguous. In setting limits (section 4.3), we shall be conservative and take this event as a candidate for having a mass of around 60 GeV.

In conclusion, with our best possible mass resolution no high mass resonance structure is visible.

4 Search for events with a high mass photon pair and fermion pair

We discuss here a search for high mass photon pairs in events with quarks or with neutrinos. Upper limits are set on $f\bar{f}\gamma\gamma$(f $= \ell, q, \nu$) production using the results of the two searches described here together with the $\ell^+\ell^-\gamma\gamma$ search of section 3.

4.1 $q\bar{q}\gamma\gamma$ events

Events are selected as hadronic events with at least two photon candidates if the total number of tracks and clusters is larger than 12 and the total energy of all the high energy isolated photon candidates is greater than 20% of the centre-of-mass energy. Electromagnetic clusters with $|\cos\theta| < 0.9$ that are detected outside the overlap region are considered as candidates for high energy photons. The cluster energy must exceed 5 GeV and the cluster shape for photons detected in the barrel must be consistent with that expected from a single electromagnetic shower using the criteria of reference [14]. After excluding tracks from reconstructed photon conversions, the photon candidate is retained if no track with momentum above 250 MeV is associated to the cluster and no additional track or cluster is found within a cone of 15° half-angle.

Three candidate events for $q\bar{q}\gamma\gamma$ are found with $m_{\gamma\gamma}$ above 40 GeV. The mass values for these candidate events are shown in Table 3 together with the isolation angles. The number of events in this mass range predicted by the Jetset 7.3 QCD Monte Carlo event generator [23] is 0.6±0.4, and for Ariadne 4.0 [24] is 3.6±1.2 after full detector simulation. These predictions include the contributions from multiple hard photon emission from quarks and the background from mis-identified hadrons (π^0,η^0 etc.). Assuming isospin conservation, the background contribution from hadrons faking at least one photon is 1 ± 1 event, estimated from the number of isolated charged particles in the data. The invariant mass distribution of the photon candidate pairs in all the selected hadronic events is shown in Figure 2. The overall detection efficiency for $e^+e^- \to q\bar{q}X$ events with X decaying to $\gamma\gamma$ and $m_X = 60$ GeV is 51±3% using the model described in section 3.

Table 3: List of $\gamma\gamma$ invariant masses for candidate $q\bar{q}\gamma\gamma$ events with $m_{\gamma\gamma} > 40$ GeV. The measured photon energies, E_γ, as well as the minimum isolation angle ψ_{min}, between the photon candidates and the charged tracks are also listed.

Event	E	F	G
$m_{\gamma\gamma}$ (GeV)	43.2 ± 1.7	59.5 ± 2.2	76.0 ± 2.6
$E_{\gamma 1}$ (GeV)	27.5	33.9	39.0
$E_{\gamma 2}$ (GeV)	17.8	27.0	37.8
ψ_{min} (°)	17.4	16.3	33.0

4.2 $\nu\bar{\nu}\gamma\gamma$ events

In this analysis a search is performed for events with no charged particles and at least two neutral clusters. We make use of the almost 4π coverage for energetic electromagnetic particles that are detected in the barrel and endcap lead-glass calorimeters and the forward detectors down to polar angles of 34 mrad.

The following pre-selection criteria which closely follow reference [16] are used:

(1) no track with more than 20 hits is found in the central detector;

(2) at least two electromagnetic clusters with an energy of more than 1 GeV are found (these clusters are considered as being photons);

(3) one photon has to be found with $|\cos\theta| < 0.8$ and a second one with $|\cos\theta| < 0.94$ (one photon is required to be in the barrel region to ensure full trigger efficiency at low energy);

(4) cosmic ray events and beam halo muons are removed by limiting the cluster extent to 300 mrad in θ and ϕ and requiring that no track segment is reconstructed in the muon chambers or the hadron calorimeter;

(5) at least one of the photons must have an associated TOF signal which is consistent within 5 ns with originating from a genuine e^+e^- interaction (if both of the highest energetic clusters have associated TOF hits then both must satisfy the timing condition), and

(6) the energy deposited in the forward detector is required to be smaller than 2 GeV.

The pre-selection efficiency is about 80% if both photons are in the barrel region and about 65% if only one photon is found in the barrel region of the detector (mainly due to the photon conversion probabilities in the central detector and coil). After these requirements only events of the type $e^+e^- \to \gamma\gamma$, $e^+e^- \to \gamma\gamma\gamma$, $e^+e^- \to e^+e^-\gamma\gamma$ and $e^+e^- \to \nu\bar{\nu}\gamma\gamma$ are expected. Moderately high mass events with two acoplanar photons can occur from $\nu\bar{\nu}\gamma\gamma$ where the two photons arise from initial state radiation : only 0.2 events with mass above 10 GeV are expected for the current data sample as evaluated using the event generator of [25].

Firstly, we search for events with exactly two photons. No additional cluster with an energy above 500 MeV is allowed in the event. The acoplanarity angle of the two clusters is required to be greater than 5°. No event with a mass above 5 GeV is found. The overall detection efficiency for $e^+e^- \to \nu\bar{\nu}X$ events with X decaying to $\gamma\gamma$ and $m_X = 60$ GeV is 56±3% using the model of section 3.

In order to be sensitive to multi-photon decays of X and insensitive to the third photon veto, we also search for events containing two or more photons. In such events then, in addition to the above acoplanarity criterion, we require that the measured missing energy transverse to the beam direction (E_T) exceeds 10 GeV. Each photon with energy above 5 GeV is required to be outside the overlap region in order to ensure a good resolution on E_T. No events are found. The efficiency calculated as above is 43±2%. The $\gamma\gamma$ systems of all four $\ell^+\ell^-\gamma\gamma$ events of L3 satisfy the above acoplanarity and missing transverse energy criteria [1].

4.3 Upper limits on $e^+e^- \to f\bar{f}X \to f\bar{f}\gamma\gamma$

In calculating the following limits we take any observed event in the ±5 GeV mass interval centred on 60 GeV as a candidate (including the ambiguous $\ell^+\ell^-\gamma\gamma$ event). The bin width matches the mass resolution of about 2 GeV and allows for some uncertainty on the central value. The error given in Table 4 is subtracted from the efficiency. The three lepton flavours are assumed to be produced equally (the limits for each flavour can be calculated separately from the quoted numbers if required). The 95% C.L. limits calculated for the $\ell^+\ell^-\gamma\gamma$ ($\ell = e, \mu, \tau$), $q\bar{q}\gamma\gamma$ and $\nu\bar{\nu}\gamma\gamma$ channels are shown in Table 4.

Using the hadronic and invisible Z^0 decay branching fractions measured at LEP [26], the quark and neutrino searches are combined to give an upper limit of 6.0×10^{-6} on $B(Z^0 \to Z^{*0}\gamma\gamma)$, more stringent than the one given in [27]. We deduce that any contribution to $\ell^+\ell^-\gamma\gamma$ events with $m_{\gamma\gamma} \approx 60$ GeV from associated production with a virtual Z^0 occurs at a branching fraction of less than 6.0×10^{-7} (95% C.L.). The four events from L3 near 60 GeV correspond to a Z^0 branching fraction to $\ell^+\ell^-\gamma\gamma$ of order 5×10^{-6} for their data-sample. This is an order of magnitude greater than the contribution from Z^{*0} which is permitted from the OPAL searches in the quark and neutrino channels.

Independent of the production mechanism, the direct search in the $\ell^+\ell^-\gamma\gamma$ channel alone shows

Table 4: List of 95% C.L. upper limits on the cross-sections for $\ell^+\ell^-\gamma\gamma$, $\nu\bar{\nu}\gamma\gamma$ and $q\bar{q}\gamma\gamma$ events with $m_{\gamma\gamma} = 60 \pm 5$ GeV based on the observed number of events for each channel (N_{obs}) and a total integrated luminosity of 43 pb^{-1}. Also listed are the 95% C.L. upper limits on the Z^0 branching fraction into these modes based on a total of 1.8×10^6 produced Z^0's. N_{CL} is the limit obtained from N_{obs} with no allowance for background and ϵ is the search efficiency together with systematic error.

Fermion type	N_{obs}	N_{CL}	ϵ	Upper limit on cross-section (pb)	Upper limit on $B(Z^0 \to f\bar{f}\gamma\gamma)$
ℓ ($\ell = e, \mu, \tau$)	1	4.74	$41 \pm 2\%$	0.28	6.8×10^{-6}
q	1	4.74	$51 \pm 3\%$	0.23	5.5×10^{-6}
ν	0	3.0	$56 \pm 3\%$	0.13	3.1×10^{-6}

no corroborating evidence for a Z^0 branching fraction of order 5×10^{-6} but can not exclude such a magnitude. The upper limit at 95 % C.L. on the branching fraction is 6.8×10^{-6}.

5 Search for anomalous production of high mass photon pairs in $e^+e^- \to \gamma\gamma\gamma$ events

If X were produced in association with a virtual photon, which could explain the $\ell^+\ell^-$ in the $\ell^+\ell^-\gamma\gamma$ events of L3 and the absence of $\nu\bar{\nu}\gamma\gamma$ events, then it may also be produced in association with a real photon leading to a final state with three photons. A significant background to this search is the QED reaction $e^+e^- \to \gamma\gamma\gamma$. This process has been studied by OPAL based on the data collected before 1991 [28] and by other experiments at LEP [29]. Only a few events have been observed and no deviations from the QED expectation were reported.

This analysis starts from a low multiplicity sample and requires that at least three electromagnetic clusters are found with energy exceeding 10% of the beam energy within the region $|\cos\theta| < 0.94$. The three most energetic clusters must be isolated from each other by at least 10°. Three-body events are selected by requiring that the energy of any additional clusters does not exceed 2.5 GeV and that the sum of the opening angles exceeds 350°. Events are accepted if they have no charged tracks or two charged tracks which can be reconstructed as a photon conversion. From the data sample of 43 pb^{-1} we find 38 events, in agreement with the expectation from QED of 36.5 ± 4.0. The prediction uses the generator of [30] with full detector simulation. The error is dominated by an assumed 10% uncertainty from higher order corrections.

In the search for the production of γX we require that the event is highly planar (the sum of the opening angles must exceed 359°) in order to justify the use of three-body kinematics for the calculation of the photon energies from the measured photon angles. This condition is satisfied by 37 events. Monte Carlo studies using full detector simulation indicate that for genuine three-body events the mass resolution using these reconstructed energies is better than 1 GeV over the entire acceptance. In order to discriminate against the strongly forward peaked QED background we require that at least one photon is reconstructed within $|\cos\theta| < 0.5$. 24 events are selected compared to an expectation from QED of 23.0 ± 2.6. The efficiency for γX production, with $m_X \approx 60$ GeV, and subsequent $X \to \gamma\gamma$ decay is estimated to be $65 \pm 2\%$ using a Monte Carlo with full detector simulation where the production angular distribution is $1 + \cos^2\theta$ and X has zero spin. The calculation of Ref.

[31] for s-channel photon exchange gives this angular distribution and yields :

$$\sigma(e^+e^- \to \gamma X)B(X \to \gamma\gamma) = \frac{8\pi\alpha}{3}\left\{\frac{1}{m_X}\left(1 - \frac{{m_X}^2}{s}\right)\right\}^3 \Gamma_X B^2(X \to \gamma\gamma)$$

The $m_{\gamma\gamma}$ distribution for each photon pairing in these 24 events is shown in figure 3 compared to the QED MC expectation. Only one entry per bin per event is plotted. Seven events have at least one photon pairing with $m_{\gamma\gamma}$ within ± 2.5 GeV of 60 GeV. This is the bin chosen by L3 to present their $\ell^+\ell^-\gamma\gamma$ data. For this search, the experimental mass resolution is much smaller than the bin size. The expected number of events from the QED reaction $e^+e^- \to \gamma\gamma\gamma$ with at least one photon pairing in this mass bin is evaluated as above to be 2.7 ± 0.4. The probability of seven or more events originating from a QED background fluctuation is 2%, so a QED fluctuation can certainly not be excluded. The following 95 % CL upper limits based on seven observed events in the presence of background are obtained using the method of Ref. [32]. We place an upper limit of 0.4 pb on $\sigma(e^+e^- \to \gamma X)B(X \to \gamma\gamma)$. The upper limit on $\Gamma_X B^2(X \to \gamma\gamma)$ is 20 MeV, evaluated for $m_X = 60 \pm 1$ GeV using the above calculation.

The kinematically constrained mass resolution for 60 GeV photon pairs in events with exactly three photons is estimated, from the full detector simulation, to be on average 300 MeV. We look for possible sub-structure near 60 GeV to search for events consistent, within our mass resolution, with a narrow resonance. We carry out two kinematic fits to these seven events : a 4C fit with four-momentum conservation as the constraints, and a 3C fit allowing for ISR in one hemisphere. The longitudinal beam spread of approximately ± 1 cm affects the precision of the polar angle measurement. The fits have been performed with the run-averaged longitudinal vertex position and the effect of the beam spread evaluated by varying this vertex by one standard deviation. The four-vectors of the seven events are given in Table 5 together with the masses reconstructed from the angles and from the 4C kinematic fit. We find that the 4C fit gives a satisfactory description of most events. The fitted masses agree well with the reconstructed masses. The 3C fit does not give a significantly better fit except possibly for event J [2].

Four events (J, K, L and N) have a mass in the interval 58.25 GeV to 60.25 GeV. This bin was chosen as being centred on the cluster of three $\ell^+\ell^-\gamma\gamma$ events from L3 that are consistent with a narrow resonance and the bin width is about ± 3 standard deviations for average events. The background expectation for this 2 GeV wide bin is 1.1 ± 0.2 which gives a probability of 2.5% for a background fluctuation. The four mass values are in accord with each other (χ^2 of 6.5 for 3 degrees of freedom) and are consistent with a mass of 59.7 ± 0.1 GeV.

6 Search for high mass photon pairs in photon-photon collisions

If a particle decays with a large partial width into two photons, then, assuming time reversal invariance, it can also be produced in photon-photon collisions. We search for a 60 GeV resonance produced in photon-photon collisions and decaying into two photons ($e^+e^- \to e^+e^-X \to e^+e^- + \gamma\gamma$). In this analysis, the same pre-selection criteria as in subsection 4.2 are used except that the restriction against energy in the forward detector is removed. We restrict the search to events with only two photons and exclude the calorimeter overlap region. Two-photon collisions are characterised by the production of events with balanced transverse energy and a longitudinally boosted system. We require that the

[2] The 4C fit is acceptable (χ^2/dof = 2.9/4) and gives $m_{12} = 58.25 \pm 0.72 \pm 1.46$ GeV where the first error is the fit error and the second the beam spread systematic. The 3C fit is better (χ^2/dof = 0.5/3) and the mass value is $m_{12} = 59.58 \pm 1.12 \pm 0.27$ GeV with $E_{ISR} = 0.45 \pm 0.3$ GeV.

Table 5: Four vector list of the $\gamma\gamma\gamma$ events with at least one photon pairing with $m_{\gamma\gamma}$ within ± 2.5 GeV of 60 GeV. The measured angles and photon energies calculated from those angles using three-body kinematics are listed. The photons are listed with the invariant mass of photons 1 and 2 nearest to 60 GeV. Note that for some events other pairings give similar masses. The reconstructed mass of photons 1 and 2, ${m_{12}}^{rec}$, and the mass found in the 4C kinematic fit, ${m_{12}}^{fit}$ are listed. The error on ${m_{12}}^{fit}$ is evaluated as the sum in quadrature of the fit error and the systematic error due to the longitudinal beam spread.

Event	H	I	J	K	L	M	N
$\sqrt{s}$ (GeV)	91.259	90.256	92.960	91.218	91.304	91.298	91.300
$E_{\gamma 1}$ (GeV)	39.8	42.7	46.2	43.7	41.4	33.4	33.5
$\cos\theta_{\gamma 1}$	−0.845	−0.247	−0.357	0.559	0.736	0.377	0.038
$\phi_{\gamma 1}$ (°)	176.5	332.6	54.7	316.1	98.5	76.1	97.5
$E_{\gamma 2}$ (GeV)	24.2	20.9	18.1	21.4	23.6	32.8	31.9
$\cos\theta_{\gamma 2}$	0.929	0.053	0.187	−0.162	−0.889	−0.833	−0.699
$\phi_{\gamma 2}$ (°)	253.4	125.0	236.8	144.0	218.5	217.1	254.8
$E_{\gamma 3}$ (GeV)	27.2	26.6	28.6	26.1	26.3	25.1	25.9
$\cos\theta_{\gamma 3}$	0.409	0.354	0.459	−0.804	−0.360	0.583	0.810
$\phi_{\gamma 3}$ (°)	17.4	175.4	233.1	125.8	300.7	290.5	312.9
${m_{12}}^{rec}$ (GeV)	57.94	57.79	57.65	59.60	59.46	61.23	59.99
${m_{12}}^{fit}$ (GeV)	57.99	57.81	58.25	59.56	59.44	61.27	59.99
	±0.16	±0.13	±1.62	±0.53	±0.17	±0.11	±0.16

photons are coplanar (acoplanarity angle $< 5°$) and acollinear (acollinearity angle $> 5°$). The expected background comes from $e^+e^- \to \gamma\gamma\gamma$ events with one of the γ's escaping undetected near the beam direction. Such three-body final states are rejected by requiring:

$$E_{\gamma\gamma\gamma} \equiv E_1 + E_2 + \sqrt{s}\left\{1 + \frac{\sin\theta_1 + \sin\theta_2}{|\sin\theta_1\cos\theta_2 + \cos\theta_1\sin\theta_2|}\right\}^{-1} < 0.95\sqrt{s},$$

where E_1 and E_2 are the energies of the two measured photons and the third term is the calculated missing energy obtained from the measured polar angles (θ_1 and θ_2) of the two photons assuming a $\gamma\gamma\gamma$ final state with the third unseen photon assigned no transverse energy. The distribution of $E_{\gamma\gamma\gamma}$ normalised to the centre-of-mass energy is shown in Figure 4(a) before this requirement is applied.

Twenty events are selected. The $m_{\gamma\gamma}$ distribution is shown in Figure 4(b). One event has a photon-pair mass of 61.4 GeV. The background from $e^+e^- \to \gamma\gamma\gamma$ is estimated, using the generator of [30] and a parametrisation of the energy resolution, to contribute 0.8 ± 0.5 events in the ± 5 GeV mass interval centred on 60 GeV.

The detection efficiency of $\gamma\gamma \to X \to \gamma\gamma$ events with $m_X = 60$ GeV is evaluated using a Monte Carlo method. The Monte Carlo is based on the equivalent photon approximation for the event generation and takes into account the detector acceptance criteria and the selection efficiency described above. The overall detection efficiency is $45 \pm 2\%$ if the X particle has spin 0 and at least $29 \pm 1\%$ for the tensor case which strongly depends on the decay angular distribution of X relative to the beam direction. The cross-section multiplied by the decay branching fraction into $\gamma\gamma$ in this approximation [33, 32] is given by :

$$\sigma(e^+e^- \to e^+e^- X)B(X \to \gamma\gamma) = \left(\frac{\alpha}{2\pi}\ln\frac{s}{4{m_e}^2}\right)^2 \frac{(2J+1)8\pi^2}{s m_X} f(\frac{m_X^2}{s})\Gamma_X B^2(X \to \gamma\gamma)$$

where

$$f(\omega) = \frac{1}{\omega}\{(2+\omega)^2 \ln\frac{1}{\omega} - 2(1-\omega)(3+\omega)\},$$

Γ_X is the total width and J is the spin of particle X. Based on the observation of one event as a candidate, we obtain 95% C.L. upper limits on $\Gamma_X B^2(X \to \gamma\gamma)$ of 2.6 MeV for $J = 0$ and 0.8 MeV for $J = 2$. The limits were evaluated for $m_X = 60 \pm 1$ GeV and take into account an assigned 10% uncertainty arising from the use of the equivalent photon approximation.

7 Search for Events with an Isolated High Momentum Lepton Pair

We search for the production of a possible resonance X, near 60 GeV, in association with an isolated high momentum e^+e^- or $\mu^+\mu^-$ pair. The non-$\gamma\gamma$ decays of X into $q\bar{q}$, $\ell^+\ell^-(\ell = e, \mu, \tau)$ and $\nu\bar{\nu}$ are considered. Tau leptons are not considered for the "non-X" lepton pair because for such topologies the mass of X can not be meaningfully estimated using the recoil mass of the non-X lepton pair. The purpose of these searches is to obtain an upper limit on $\sigma_{\ell^+\ell^-X}(1 - B(X \to \gamma\gamma))$ by searching for all possible decay modes other than $\gamma\gamma$. This can be combined with the $\Gamma_X B^2(X \to \gamma\gamma)$ upper limit obtained from the search for X production in photon-photon collisions to extract information on Γ_X.

7.1 Search for $e^+e^- \to \ell^+\ell^- q\bar{q}$

This event topology is the same as for the standard model Higgs boson production associated with a lepton pair from a virtual Z^0. The selection criteria for this topology are similar to those of the previous Higgs search paper by OPAL [34]. The invariant mass of the two leptons is required to be greater than 15 GeV, and the invariant mass of the hadronic system must exceed 25 GeV. The invariant mass of the hadronic system is calculated using the charged particle momenta, electromagnetic and hadron calorimeter energies and avoiding the double counting of energies [34]. No events survived after all the cuts. The detection efficiency of the standard model Higgs boson of mass 60 GeV accompanied by an e^+e^- or $\mu^+\mu^-$ pair is $32 \pm 2\%$.

7.2 Search for $e^+e^- \to \ell^+\ell^-\ell^+\ell^-$

This topology was previously studied in the search for lepton pair events associated with an additional charged particle pair ($\ell^+\ell^-$V events) [37] from the 1990 and 1991 data sample. Events are required to have four and only four charged particles within the polar angle region of $|\cos\theta| < 0.9$. Three of the four charged particles must have momentum greater than 5 GeV, the remaining one must have a momentum greater than 1 GeV and the charge must balance. The opening angle of any pair of the four charged particles must be greater than 15°. At least two of the four charged particles must be associated with clusters in the electromagnetic calorimeter. Sixteen events are selected. The number of background events expected from electroweak processes is 23.9 ± 2.0, which is estimated by using the Monte Carlo event generator of Daverveldt [35] with full detector simulation. For each event, there are two sets of possible $\ell^+\ell^-$ combinations. The higher $\ell^+\ell^-$ recoil mass of each set is plotted in Figure 5 together with the Monte Carlo prediction. In order to search for a resonance state X with mass of approximately 60 GeV, we require that one of these higher recoil masses is within ±5 GeV of 60 GeV. Two of the 16 events are retained. The expected number of events from electroweak processes is 5.7 ± 1.1. The overall detection efficiency of $e^+e^- \to e^+e^-X$ or $\mu^+\mu^-X$ events with X decaying to $\ell^+\ell^-$ was calculated to be $49 \pm 2\%$ where the decay branching fractions of X into each lepton flavour are assumed to be equal for simplicity.

7.3 Search for $e^+e^- \to \ell^+\ell^-\nu\bar{\nu}$

Previously, we have studied this event topology in a general search for acoplanar particle pairs [19] and in a search for light Higgs bosons [36]. In this analysis, events with this topology are selected by requiring there to be two and only two charged particles. Each one must be within $|\cos\theta| < 0.9$ and have a momentum greater than 5 GeV. The charged particles must be isolated by 15° and have an acoplanarity angle exceeding 15°. In order to strengthen this criterion in the forward region, the acollinearity angle must exceed 20°. No electromagnetic calorimeter clusters unassociated to charged particles with energy above 1.5 GeV nor energy deposition in the forward detector exceeding 2 GeV are allowed. No events are selected. The overall detection efficiency for $e^+e^- \to e^+e^-X$ or $\mu^+\mu^-X$ events with $m_X = 60$ GeV and X decaying to $\nu\bar{\nu}$ is calculated as above to be $49 \pm 2\%$.

7.4 Upper limit on the decay width of the possible resonance X

In this subsection, an upper limit on Γ_X is calculated as a function of the cross-section of $\ell^+\ell^-\gamma\gamma$ events arising from the production of a narrow resonance X. The decay modes $X \to q\bar{q}$, $X \to \ell^+\ell^-(\ell = e, \mu, \tau)$, $X \to \nu\bar{\nu}$ and $X \to \gamma\gamma$ are denoted by $i = 1, 2, 3$ and 4, respectively. We denote each decay branching fraction of X by B_i, and the total cross-section for $e^+e^- \to \ell^+\ell^-X(\ell = e, \mu)$ by $\sigma_{\ell^+\ell^-X}$.

Firstly, an upper limit on $(B_1 + B_2 + B_3)\sigma_{\ell^+\ell^-X}$ is calculated based on the number of events observed for each channel (N_i^{obs}) and the number of background events expected (N_i^{bkg}). If N_i^{bkg} exceeds N_i^{obs}, N_i^{bkg} is set equal to N_i^{obs} for a conservative estimate. The number of events expected is calculated as $N_i^{exp} = \epsilon_i L \sigma_{\ell^+\ell^-X} B_i$ for each mode i, where ϵ_i is the detection efficiency and L is the integrated luminosity of 43 pb^{-1}. All the efficiencies are calculated assuming the standard model Higgs boson production with mass of 60 GeV associated with e^+e^- or $\mu^+\mu^-$. The one standard deviation systematic errors of the efficiencies are subtracted from ϵ_1, ϵ_2 and ϵ_3. The efficiency variation due to model dependence (see Section 3.1) is not included in the systematic error. The upper limit on $(B_1 + B_2 + B_3)\sigma_{\ell^+\ell^-X}$ is obtained by varying $B_i\sigma_{\ell^+\ell^-X}$ (i =1,2,3) independently under the following condition corresponding to 95% C.L. The worst case is used to set the limit.

$$\frac{\sum_{n_1,n_2,n_3} \prod_{i=1}^{3} \exp(-N_i^{exp} - N_i^{bkg})(N_i^{exp} + N_i^{bkg})^{n_i}/n_i!}{\sum_{n_1,n_2,n_3} \prod_{i=1}^{3} \exp(-N_i^{bkg})(N_i^{bkg})^{n_i}/n_i!} = 0.05,$$

where the sum is over all the sets of non-negative integers n_1, n_2, n_3 which satisfy

$$\sum_{i=1}^{3} \frac{n_i}{\epsilon_i L} \leq \sum_{i=1}^{3} \frac{N_i^{obs}}{\epsilon_i L}.$$

The resulting limit is $(B_1 + B_2 + B_3)\sigma_{\ell^+\ell^-X} < 0.27$ pb at 95% C.L. The equivalent upper limit on $(B_1 + B_2 + B_3)B(Z^0 \to \ell^+\ell^-X)$ is 6.5×10^{-6}. The values used for the calculation of these limits are listed in Table 6 together with the upper limits for each individual decay mode.

A 95% C.L. lower limit on $B_4 \equiv B(X \to \gamma\gamma)$ is then calculated for a given cross-section of $\ell^+\ell^-\gamma\gamma(\ell = e, \mu)$ events ($\sigma_{\ell^+\ell^-\gamma\gamma} \equiv \sigma_{\ell^+\ell^-X}B_4$) assuming that X decays either into $q\bar{q}$, $\ell^+\ell^-$, $\nu\bar{\nu}$ or $\gamma\gamma$ ($B_1 + B_2 + B_3 + B_4 = 1$). Finally, the upper limit on the decay width (Γ_X) is calculated using the lower limit on B_4 and the upper limit on $\Gamma_X B_4^2$ described in section 6, for a given $\ell^+\ell^-\gamma\gamma$ cross section. The excluded Γ_X region as a function of $\sigma_{\ell^+\ell^-\gamma\gamma}$ is shown in Figure 6 for both $J = 0$ and $J = 2$. Also shown is the upper limit at 95% C.L. on $\sigma_{\ell^+\ell^-\gamma\gamma}(\ell = e, \mu)$ of 0.24 pb calculated from the direct search in the electron and muon channels. The ambiguous $e^+e^-\gamma\gamma$ event is considered as a candidate and the limit has been obtained using the average efficiency of $50 \pm 3\%$ evaluated from

Table 6: List of 95% C.L. upper limits on the $\ell^+\ell^-\mathrm{X}(\ell = \mathrm{e}, \mu)$ cross-section multiplied by branching ratio (B_i) of each mode i. Also listed are the 95% C.L. upper limits on $B(\mathrm{Z}^0 \to \ell^+\ell^- X)B_i(\ell = \mathrm{e}, \mu)$. The values in this table are used to calculate a combined limit on $(B_1 + B_2 + B_3)\sigma_{\ell^+\ell^-\mathrm{X}}$. N_{bkgd} is set equal to N_{obs} if N_{bkgd} exceeds N_{obs}. The efficiencies together with the one standard deviation errors are quoted. This error is subtracted in the limit evaluation.

X Decay mode	N_{obs}	N_{bkgd}	ϵ	Upper limit on $\sigma_{\ell^+\ell^-\mathrm{X}} \cdot B_i$ (pb)	Upper limit on $B(Z^0 \to \ell^+\ell^-\mathrm{X})B_i$
(1) $\mathrm{q\bar{q}}$	0	-	$32 \pm 2\%$	0.23	5.5×10^{-6}
(2) $\ell^+\ell^-$ $(\ell = \mathrm{e}, \mu, \tau)$	2	5.7	$49 \pm 2\%$	0.24	5.8×10^{-6}
(3) $\nu\bar{\nu}$	0	-	$49 \pm 2\%$	0.15	3.6×10^{-6}

section 3.1. A cross-section of 0.05 pb corresponds to the production of one detectable $\ell^+\ell^-\gamma\gamma$ event per LEP experiment (assuming data-samples of 40 pb^{-1} with a 50% efficiency).

One concludes that Γ_{X} is limited to be less than 110 MeV at 95% C.L. for $\ell^+\ell^-\gamma\gamma(\ell = \mathrm{e}, \mu)$ cross-sections greater than 0.05 pb. This limit assumes that the $\ell^+\ell^-\mathrm{X}$ cross-section is approximately constant in the $\sqrt{s}$ region where the data were taken (± 3 GeV around the Z^0 peak). The corresponding limit as a function of $B(\mathrm{Z}^0 \to \ell^+\ell^-\gamma\gamma)(\ell = \mathrm{e}, \mu)$ can also be obtained from Figure 6 in the case that the production process is predominantly via the Z^0. These upper limits on Γ_{X} are smaller than the mass resolution expected for any of the four LEP detectors.

8 Summary

We have analysed a data sample, collected between 1990 and 1992, to search for events with a pair of photons with a high mass. The data sample corresponds to a total integrated luminosity of 43 pb^{-1} or to roughly 1.8 million produced Z^0's.

Four $\ell^+\ell^-\gamma\gamma$ events with a photon pair mass above 40 GeV are found. No clustering of $m_{\gamma\gamma}$ is observed at large masses. The number of $\mu^+\mu^-\gamma\gamma$ events observed is 29 with $m_{\gamma\gamma}$ above 10 GeV and two with $m_{\gamma\gamma}$ above 40 GeV. These numbers are consistent with the YFS3 MC prediction of 22.6 ± 1.2 ($m_{\gamma\gamma} > 10$ GeV) and 1.2 ± 0.3 ($m_{\gamma\gamma} > 40$ GeV). No events are directly measured to be consistent with a mass of around 60 GeV. It should be noted that one event which is not fully reconstructed may be consistent with such a mass but that the interpretation of this event is ambiguous.

Three hadronic events with two isolated photon candidates are found with mass above 40 GeV with no obvious resonance structure. No event without tracks and two or more acoplanar photons with missing transverse energy and a mass of more than 5 GeV is found. The search for high mass photon pairs near 60 GeV in the neutrino and hadronic channel limits the branching ratio $B(\mathrm{Z}^0 \to \mathrm{Z}^{*0}\gamma\gamma)$ to 6.0×10^{-6} at 95% C.L. Therefore, any anomalous production of $\ell^+\ell^-\gamma\gamma(\ell = \mathrm{e}, \mu, \tau)$ events where the lepton pair originates from a virtual Z^0 occurs with $B(\mathrm{Z}^0 \to \mathrm{Z}^{*0}\gamma\gamma \to \ell^+\ell^-\gamma\gamma) < 6.0 \times 10^{-7}$.

Thirty-eight events of the type $\mathrm{e^+e^-} \to \gamma\gamma\gamma$ have been detected. The overall production rate is in good agreement with the expectation from QED (36.5 ± 4.0). In a search for $\gamma\mathrm{X}$ production, with X decaying to $\gamma\gamma$, seven events are found with at least one photon pairing with a mass within ± 2.5 GeV of 60 GeV. The expectation from QED is 2.7 ± 0.4. The probability of seven or more events originating from a QED background fluctuation is 2%. Four of these events are measured within a bin of ± 1 GeV centred on 59.25 GeV : the corresponding probability of a background fluctuation is 2.5%.

In a search for the production in two-photon collisions of a 60 GeV resonance X decaying to two photons, we set an upper limit on $\Gamma_X B^2(X \to \gamma\gamma)$ of 2.6 MeV at 95% CL, assuming a spin 0 resonance. We also looked for $\ell^+\ell^- X(\ell = e, \mu)$ events, where X decays into either $q\bar{q}$, $\ell^+\ell^-(\ell = e, \mu, \tau)$ or $\nu\bar{\nu}$. No indication of a 60 GeV resonance is seen in these modes. Combining these last two searches, upper limits on Γ_X as a function of $\ell^+\ell^-\gamma\gamma$ cross-section and Z^0 branching fraction are set.

Acknowledgements

It is a pleasure to thank the SL Division for the efficient operation of the LEP accelerator, the precise information on the absolute energy, and their continuing close cooperation with our experimental group. In addition to the support staff at our own institutions we are pleased to acknowledge the
Department of Energy, USA,
National Science Foundation, USA,
Texas National Research Laboratory Commission, USA,
Science and Engineering Research Council, UK,
Natural Sciences and Engineering Research Council, Canada,
Fussefeld Foundation,
Israeli Ministry of Energy and Ministry of Science,
Minerva Gesellschaft,
Japanese Ministry of Education, Science and Culture (the Monbusho) and a grant under the Monbusho International Science Research Program,
German Israeli Bi-national Science Foundation (GIF),
Direction des Sciences de la Matière du Commissariat à l'Energie Atomique, France,
Bundesministerium für Forschung und Technologie, Germany,
National Research Council of Canada,
A.P. Sloan Foundation and Junta Nacional de Investigação Científica e Tecnológica, Portugal.

References

[1] L3 Collab., O. Adriani et al., Phys. Lett. **B295** (1992) 337.

[2] S. Jadach and B.F.L. Ward, Phys. Lett. **B274** (1992) 470.

[3] L3 Collab., O. Adriani et al., CERN-PPE/93-31, submitted to Phys. Rep.

[4] M. Martinez and R. Miquel, CERN-PPE/92-211, submitted to Phys. Lett. **B** ;
K. Kolodziej, F. Jegerlehner and G.J van Oldenborgh, PSI Report No. PSI-PR-93-01 Jan. 1993;
J. Fujimoto et al., KEK Report No. P 92-195. Feb. 1993;
A. Ballestrero, E. Maina, and S. Moretti, Univ. of Turin Report No. DFTT 4/93, Feb. 1993.

[5] Y.-H. Chang, Proceedings of the XXVIIIth Rencontre de Moriond, March 1993. In preparation.

[6] VENUS Collab., K. Abe et al., Phys. Lett. **B302** (1993) 119;
TOPAZ Collab., K. Abe et al., KEK Report No. P 92-205. Feb. 1993;
AMY Collab., K.L. Sterner et al., Virginia Polytechnic Institute, Report No. VPI-IHEP-93-2.

[7] R. Garisto and J.N. Ng, TRIUMF Report No. TRI-PP-92-124, Dec. 1992.

[8] V. Barger, N.G. Deshpande, J.L. Hewett and T.G. Rizzo, Argonne National Lab. Report No. ANL-HEP-PR-92-102, Nov. 1992.

[9] G. Cvetic, M. Nowakowski and Y.-L. Wu, Univ. Dortmund Report No. DO-TH/92-24, Dec. 1992.

[10] C.Q. Geng, K. Whisnant and B.-L. Young, Iowa State Univ. Report No. IS-J 4917, Jan. 1993.

[11] K. Kang, I.G. Knowles and A.R. White, ANL-HEP-PR-93-4, Jan. 1993.

[12] V. Lubicz, Univ. of Rome "La Sapienza" Report No. ROM-P 925, Jan. 1993.

[13] K. Hagiwara, S. Matsumoto and M. Tanaka, KEK Report No. KEK-TH-353, Feb. 1993.

[14] OPAL Collab., M. Z. Akrawy et al., Phys. Lett. **B246** (1990) 285;
OPAL Collab., P. D. Acton et al., CERN-PPE/92-215, submitted to Z. Phys. **C**.

[15] OPAL Collab., P. D. Acton et al., Phys. Lett. **B273** (1991) 338.

[16] OPAL Collab., M. Z. Akrawy et al., Z. Phys. **C50** (1991) 373.

[17] OPAL Collab., M. Ahmet et al., Nucl. Instrum. and Meth. **A305** (1991) 275.

[18] M. Arignon et al., Nucl. Instrum. and Meth. **A313** (1992) 103.

[19] OPAL Collab., M.Z. Akrawy et al., Phys. Lett. **B240** (1990) 261.

[20] OPAL Collab., G. Alexander et al., Z. Phys. **C52** (1991) 175.

[21] J. Allison et al., Nucl. Instrum. and Meth. **A317** (1992) 47.

[22] F. A. Berends and R. Kleiss, Nucl. Phys. **B260**(1985) 32.

[23] T. Sjöstrand, Comp. Phys. Comm. **39** (1986) 347.

[24] U. Peterson, LU-TP 88-5 (1988); U. Peterson and L. Lönnblad LU TP 88-15 (1988); L. Lönnblad LU TP 89-10 (1989).

[25] F. A. Berends et al., Nucl. Phys. **B301** (1988) 583;
R. Miquel, C. Mana and M. Martinez, Z. Phys. **C48** (1990) 309.
The high mass expectations are calculated in M. Martinez and R. Miquel in Ref. [4].

[26] The LEP Collaborations, Phys. Lett. **B276** (1992) 247.

[27] L3 Collab., O. Adriani et al., Phys. Lett. **B292** (1992) 472.

[28] OPAL Collab., M.Z. Akrawy et al., Phys. Lett. **B257** (1991) 531.

[29] DELPHI Collab., P. Abreu et al., Phys. Lett. **B268** (1991) 296;
L3 Collab., B. Adeva et al., Phys. Lett. **B288** (1992) 404.

[30] F. A. Berends and R. Kleiss, Nucl. Phys. **B186** (1981) 22.

[31] Y. Kurihara, private communication.

[32] Particle Data Group, K. Hikasa et al., Phys. Rev. **D45** (1992) 1.

[33] V.M. Budnev et al., Phys. Rep. **15C** (1975) 181.

[34] OPAL Collab., M. Z. Akrawy et al., Phys. Lett. **B253** (1991) 511.

[35] F.A. Berends, P.H. Daverveldt and R. Kleiss, Nucl. Phys. **B253** (1985) 421; P.H. Daverveldt, Thesis, Rijksuniversiteit Leiden (unpublished).

[36] OPAL Collab., M. Z. Akrawy et al., Phys. Lett. **B251** (1990) 211.

[37] OPAL Collab., P. D. Acton et al., Phys. Lett. **B287** (1992) 389.

Figure Captions

Figure 1: (a) Invariant mass $m_{\gamma\gamma}$ of isolated photon pairs in lepton pair events. (b) Invariant mass $m_{\gamma\gamma}$ of isolated photon pairs in muon pair events (points with error bars) together with the expectation of the YFS3 Monte Carlo (histogram). The direct mass measurement from the calorimeter is shown.

Figure 2: Invariant mass $m_{\gamma\gamma}$ of pairs of isolated photon candidates in hadronic events.

Figure 3: Invariant mass $m_{\gamma\gamma}$ of each of the three photon-photon combinations in the 24 $e^+e^- \to \gamma\gamma\gamma$ events where the mass has been reconstructed using three-body kinematics. The data (points with error bars) are compared with the QED prediction (histogram) using the Berends and Kleiss Monte Carlo. For events where more than one photon-photon combination is measured in the same bin only one entry per event is shown for that bin.

Figure 4: (a) The distribution of $E_{\gamma\gamma\gamma}$ normalised to the centre-of-mass energy for candidate events for two-photon production of a high mass state before cutting on this quantity. (b) The invariant mass distribution for the two-photon production candidates.

Figure 5: The distribution of $\ell^+\ell^-$ recoil mass for $\ell^+\ell^-\ell^+\ell^-$ events (points with error bars) together with the electroweak prediction estimated from the Daverveldt Monte Carlo (histogram). The higher recoil mass for each set of two possible $\ell^+\ell^-$ combinations is plotted (two combinations per event).

Figure 6: The upper limit on Γ_X at 95% C.L. for $J = 0$ and $J = 2$ as a function of the assumed cross section of $\ell^+\ell^-\gamma\gamma(\ell = e, \mu)$ events or equivalently (upper abscissa) as a function of assumed Z^0 branching fraction to $\ell^+\ell^-\gamma\gamma(\ell = e, \mu)$. The upper limit on $\sigma_{\ell^+\ell^-\gamma\gamma}(\ell = e, \mu)$ at 95% C.L. of 0.24 pb is also shown.

Figure 1

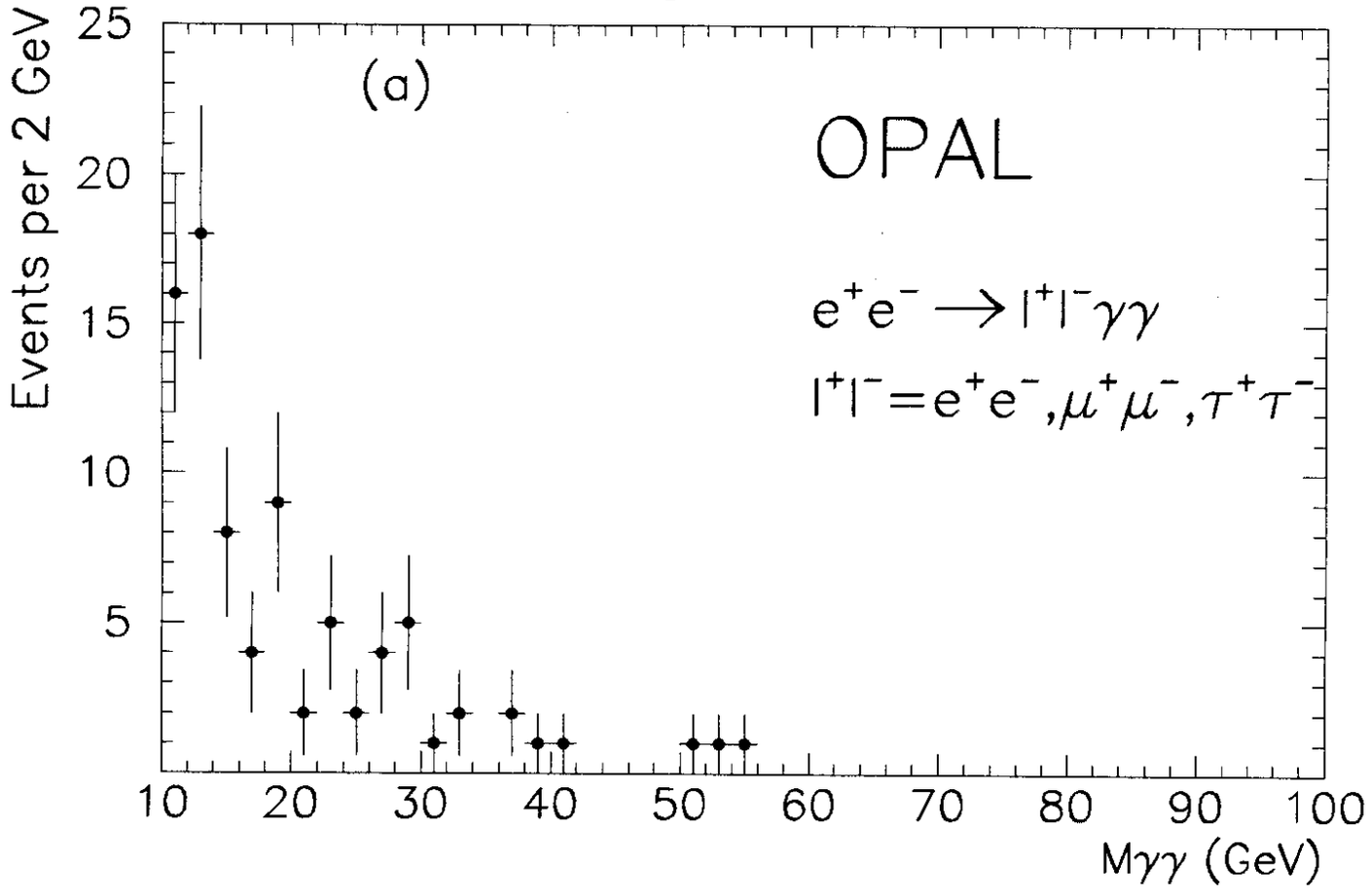
(a)
OPAL
$e^+e^- \rightarrow l^+l^-\gamma\gamma$
$l^+l^- = e^+e^-, \mu^+\mu^-, \tau^+\tau^-$
Events per 2 GeV
25
20
15
10
5
10
20
30
40
50
60
70
80
90
100
Mγγ (GeV)

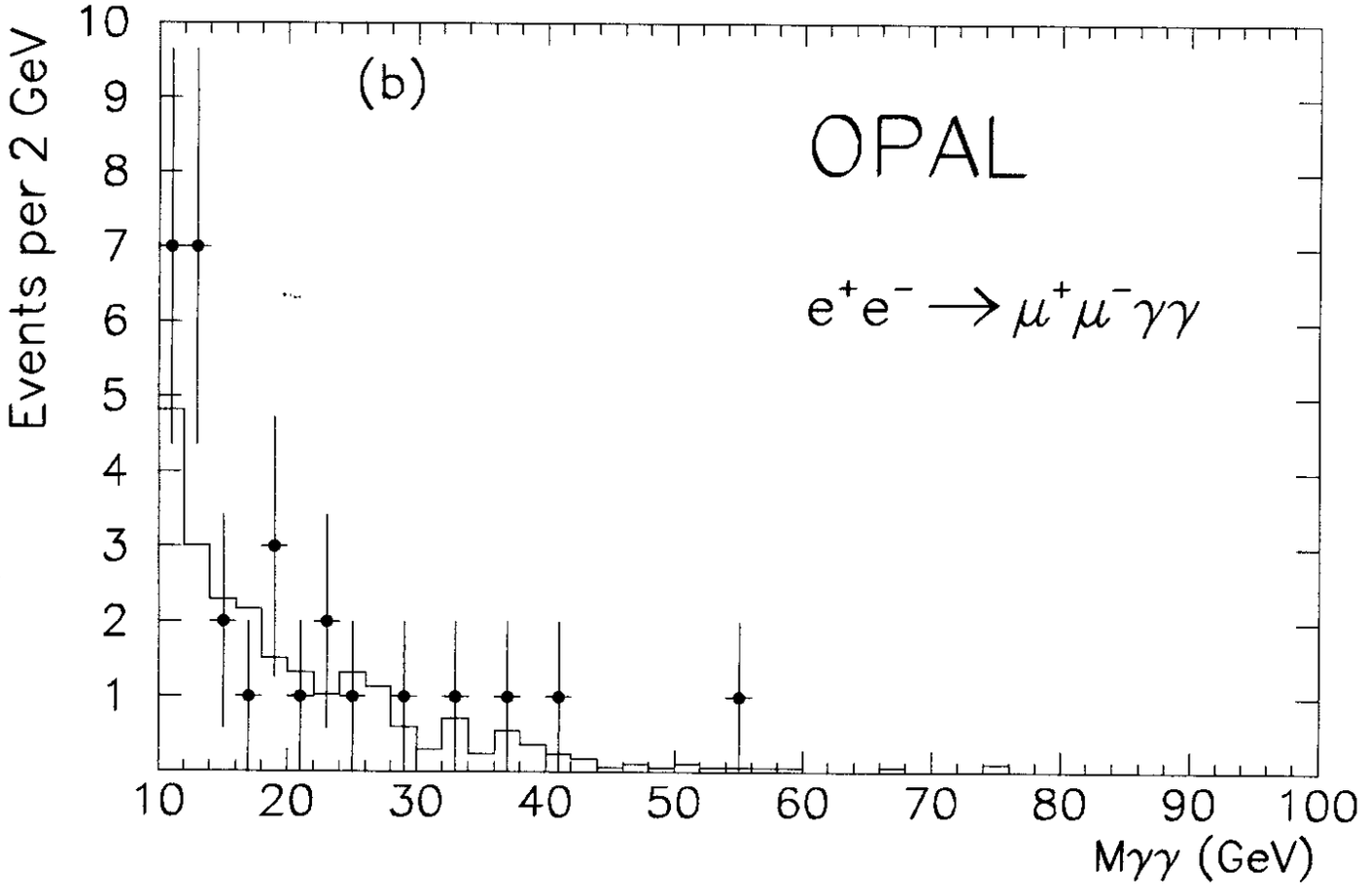
(b)
OPAL
$e^+e^- \rightarrow \mu^+\mu^-\gamma\gamma$
Events per 2 GeV
10
9
8
7
6
5
4
3
2
1
10
20
30
40
50
60
70
80
90
100
Mγγ (GeV)

Figure 2

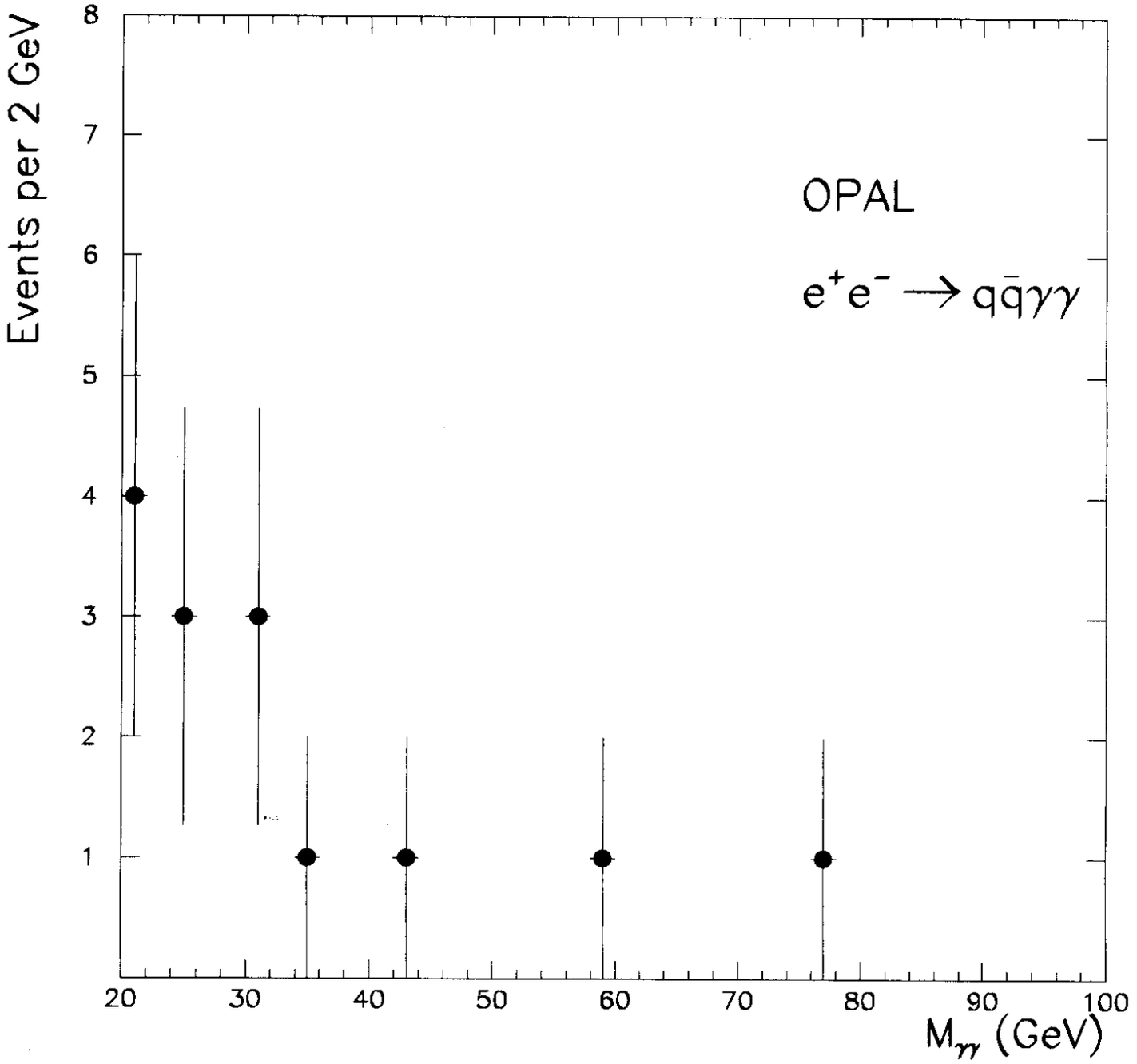
Events per 2 GeV
8
7
6
5
4
3
2
1
OPAL
$e^+e^- \rightarrow q\bar{q}\gamma\gamma$
20
30
40
50
60
70
80
90
100
$M_{\gamma\gamma}$ (GeV)

Figure 3

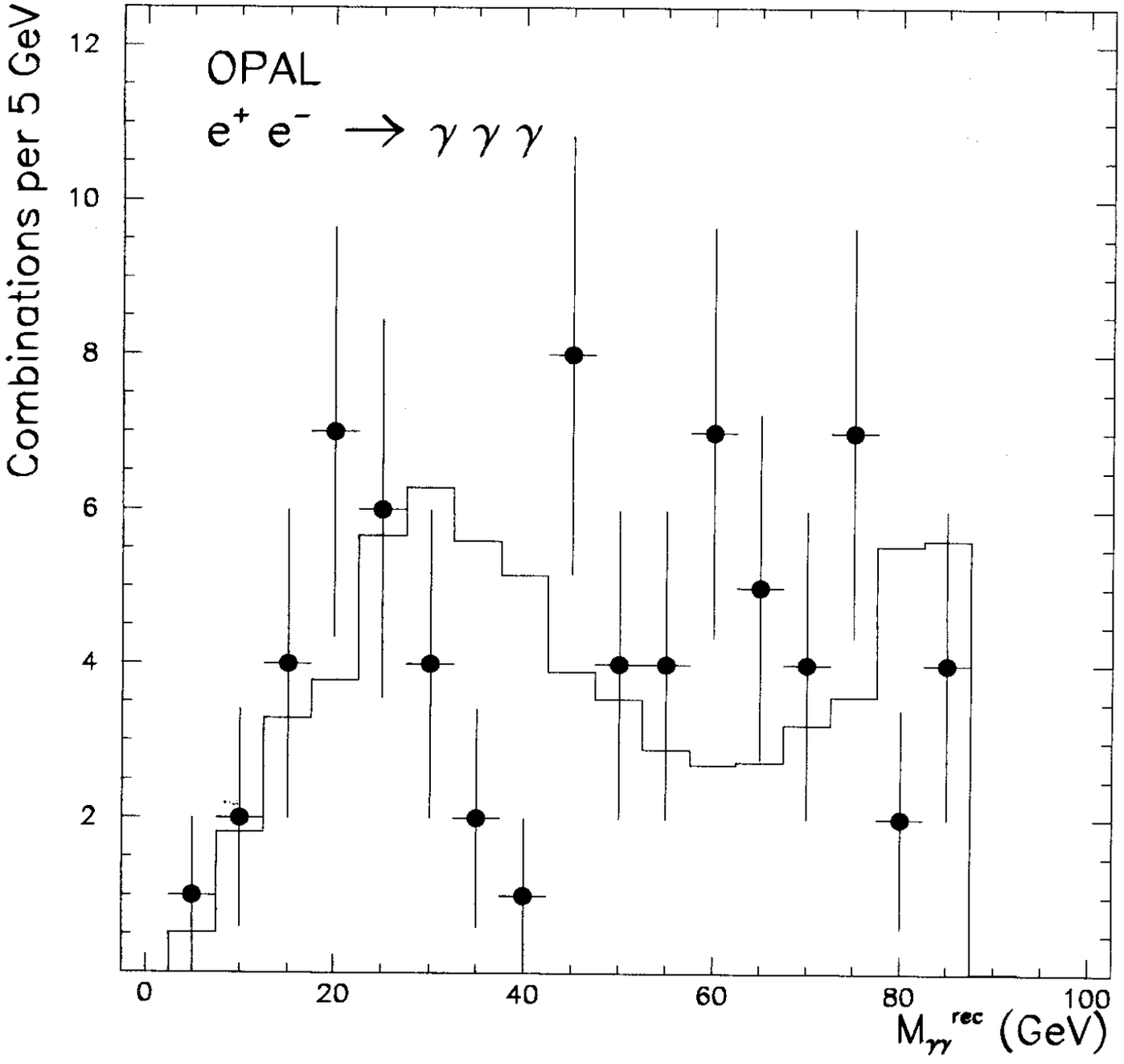
OPAL
$e^+ e^- \rightarrow \gamma\gamma\gamma$
Combinations per 5 GeV
12
10
8
6
4
2
0
20
40
60
80
100
$M_{\gamma\gamma}^{rec}$ (GeV)

Figure 4

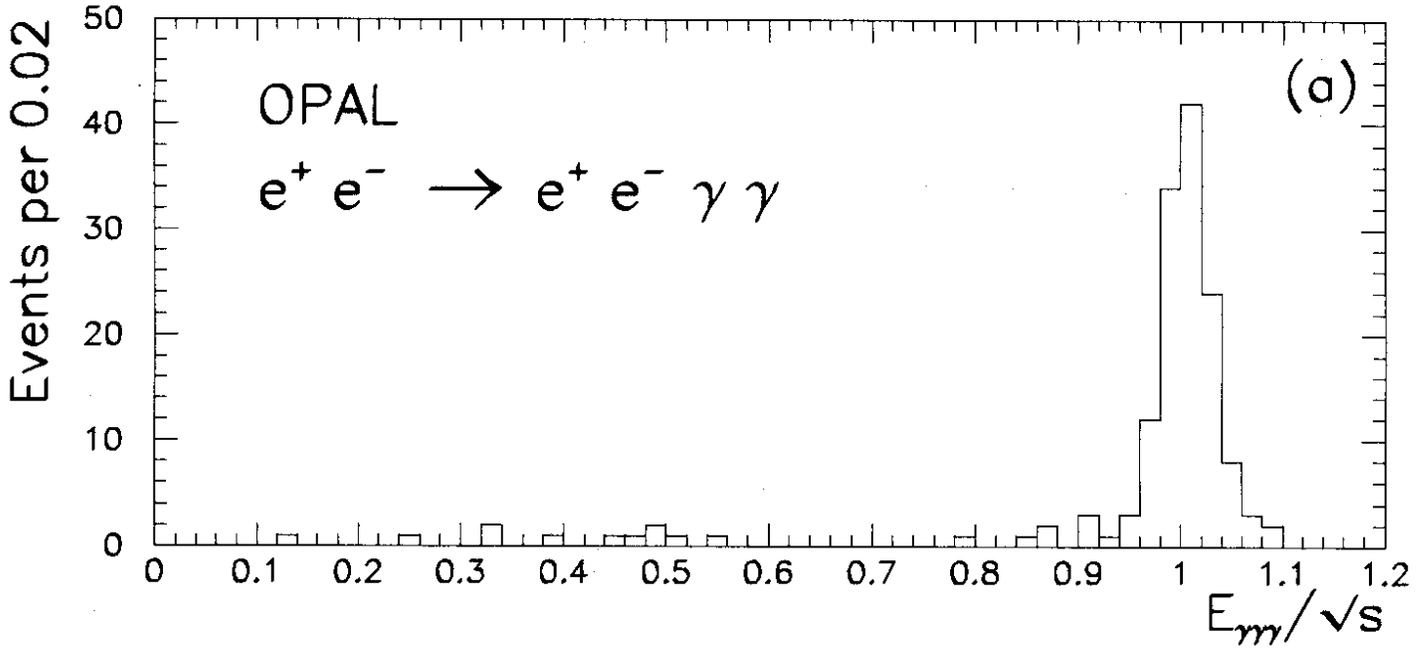
OPAL
$e^+ e^- \rightarrow e^+ e^- \gamma\gamma$
(a)
Events per 0.02
$E_{\gamma\gamma}/\sqrt{s}$

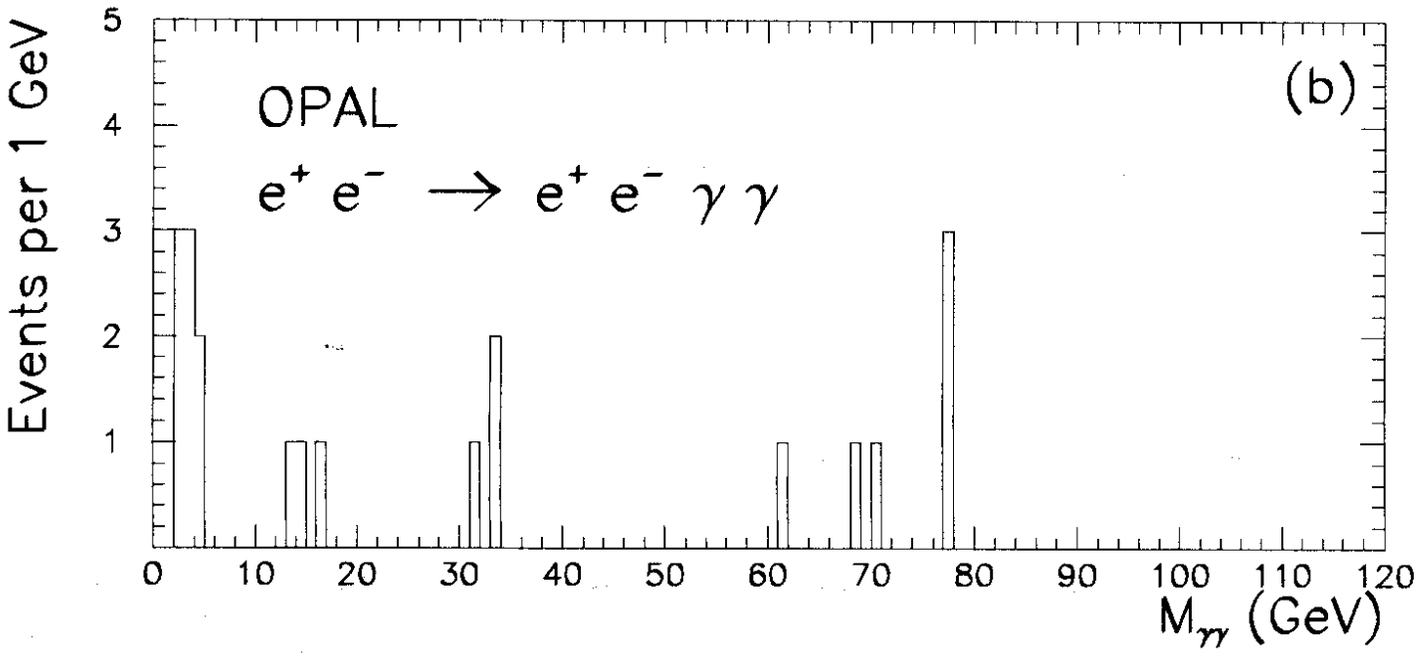
OPAL
$e^+ e^- \rightarrow e^+ e^- \gamma\gamma$
(b)
Events per 1 GeV
$M_{\gamma\gamma}$ (GeV)

Figure 5

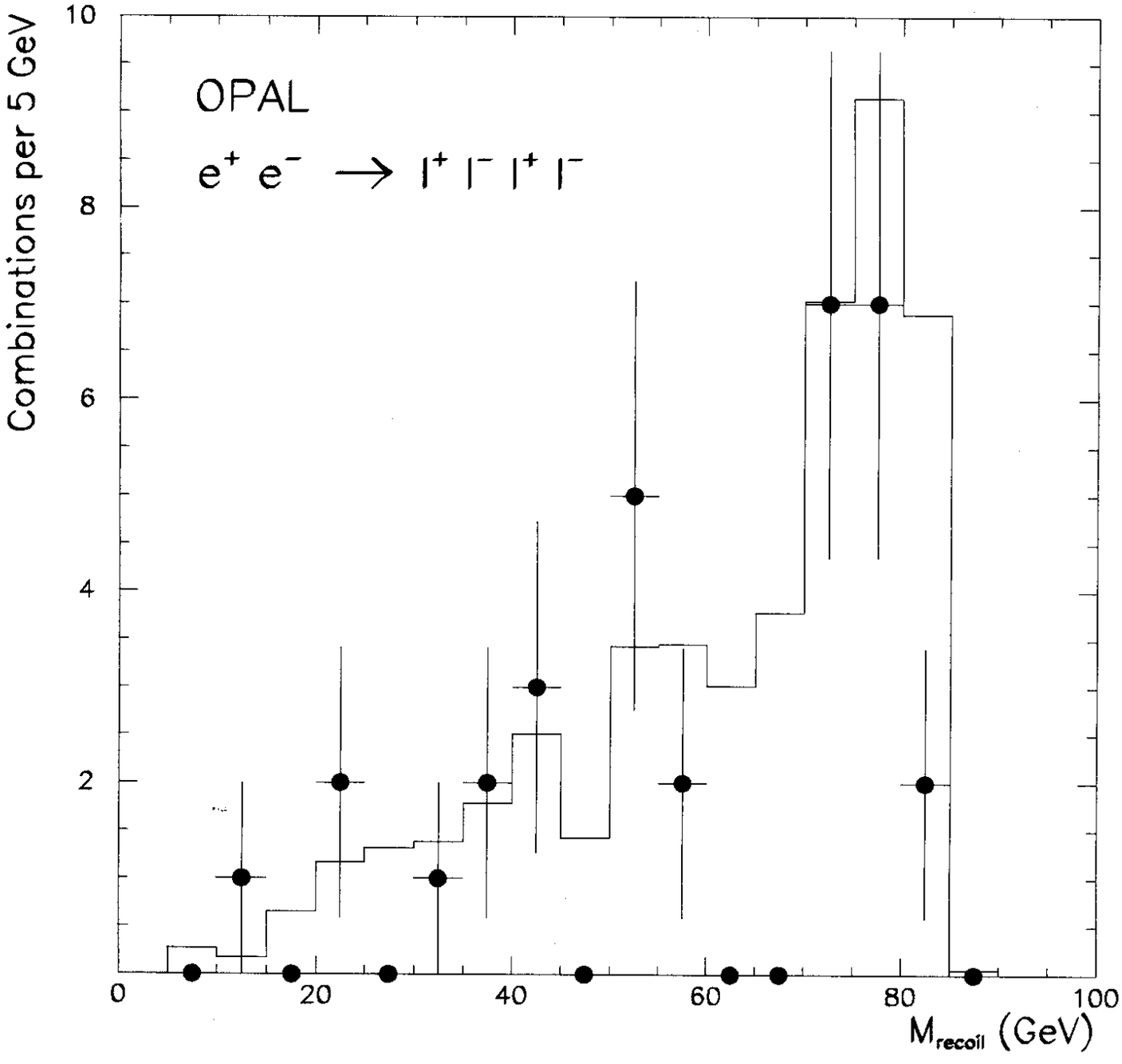
OPAL
$e^+ e^- \rightarrow l^+ l^- l^+ l^-$
Combinations per 5 GeV
10
8
6
4
2
0
20
40
60
80
100
M_{recoil} (GeV)

Figure 6

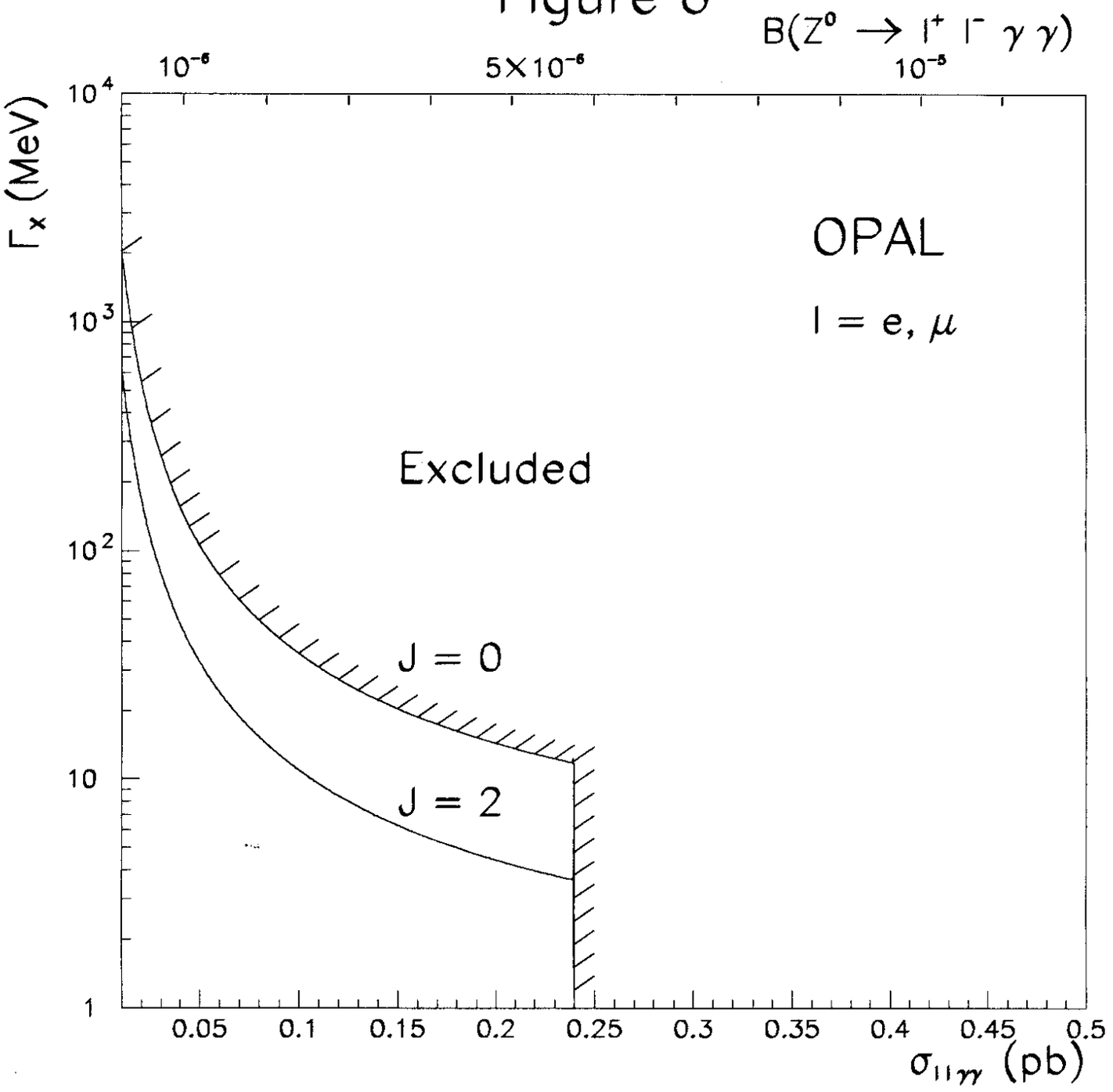
B(Z⁰ → l⁺ l⁻ γ γ)
10⁻⁶
5×10⁻⁶
10⁻⁵
F_x (MeV)
10⁴
10³
10²
10
1
OPAL
l = e, μ
Excluded
J = 0
J = 2
0.05
0.1
0.15
0.2
0.25
0.3
0.35
0.4
0.45
0.5
σ_llγγ (pb)